STUDIES OF FREE RADICALS AT 4.2°K BY ELECTRON PARAMAGNETIC RESONANCE

Thesis by

Terry Cole

In Partial Fulfillment of the Requirements

For the Degree of

Doctor of Philosophy

California Institute of Technology

Pasadena, California

1958

ACKNOWLEDGEMENTS

The author wishes to thank Professor Don M. Yost for his guidance and friendship and for the freedom he has allowed in the pursuit of this research.

This research was carried out as a joint undertaking with Mr. John T. Harding of the Physics Department; the help and cooperation of his advisor, Professor John R. Pellam is gratefully acknowledged. I wish also to thank Dr. Harden M. McConnell for his discussion of several theoretical aspects of this work.

To the Newmont Mining Company, the National Science Foundation and the Sloan Fund, acknowledgement is made for their support of this research and to the Dupont Company, the U. S. Rubber Company and California Institute of Technology for their fellowships.

ABSTRACT

Electron paramagnetic resonance spectra have been observed from the products of gaseous microwave electric discharges frozen at 4.2°K. The gases investigated were N_2 and NH_3.

The spectrum of the frozen nitrogen discharge products plainly indicates the presence of atomic nitrogen whose half life in the solid is greater than ten hours. Dilution of the nitrogen in an inert matrix of argon is found to cause considerable line broadening. When the nitrogen discharge products are passed over mercury prior to condensation, a complex spectrum of 11 lines is obtained.

The spectrum of NH_3 discharge products indicates the presence of atomic nitrogen and hydrogen. Data concerning the presence of NH and NH_2 radicals are not conclusive.

A description of the apparatus and techniques developed for these experiments is included.

TABLE OF CONTENTS

INTRODUCTION

Trapping of reactive chemical species by means of low temperatures is a relatively old technique. When such species are trapped from a gas discharge, as in the present experiments, it is often difficult to identify them since direct chemical tests are infeasible. Identification has usually been made by means of infra red spectroscopy or static susceptibility measurements. With the advent of electron paramagnetic resonance (EPR) spectroscopy it has become possible to make a far more definitive analysis of the free radicals present. Obtaining an EPR spectrum from a condensed discharge is positive proof of the presence of free radicals and the hyperfine multiplets and line widths can be used to determine the groups present and the type of matrix in which they are imbedded.

The two materials investigated were nitrogen and ammonia. Apparatus and techniques used in their study are described in the following section. A brief review of the work on the discharge products of these compounds is given followed by the results. No account of the fundamentals of EPR will be given since they have been covered fully in a number of review articles (1,2,3) and books (4,5).

EXPERIMENTAL APPARATUS

Observation of the EPR spectra of free radicals trapped at low temperatures required a three part apparatus: a system for dissociating the sample gas, a means for condensing and maintaining the gas at a low temperature and lastly, an EPR spectrometer to observe the peaks and valleys of the resonance spectrum. Figures 2 and 7 are photographs of the assembled equipment. A detailed description of its operation follows.

Gas Dissociation Apparatus. A gas dissociation apparatus similar to that described by Broida and Bass (6) (figs. 1 and 4) was constructed. The sample gas entered through a pressure reduction valve from a high pressure cylinder or in the case of ammonia, the gas was contained in a plastic beach ball. Two stopcocks regulated the flow to the dissociation chamber--the gas being drawn through the apparatus by a mechanical vacuum pump. A side arm, downstream from the dissociation chamber, was fitted with a large stopcock to control the flow of dissociated gas to the sample cavity. Energy for dissociation of the gas was provided by a Raytheon medical diathermy device (fig. 2). The 2450mc magnetron in this unit was connected through a coaxial cable to a rectangular cavity operating in the TE_{012} mode. The b dimension of the cavity was tapered in order to increase the electric field strength. A slot cut

in the narrow end of the cavity allowed the dissociation tube to pass through the cavity parallel to the E field at a point of maximum field strength. When in operation the dissociation tube required cooling to prevent softening of the pyrex tubing through dielectric heating. To do this a coaxial collar was placed around the dissociation chamber through which air was forced during a run. The side arm was attached through a ball and socket joint to a section of 9 mm pyrex tubing sealed into the waveguide that formed arm 3 of the microwave bridge (figs. 3 and 5). This tubing extended downward inside the waveguide approximately 1 m to the iris of the sample cavity at which point it was narrowed to 4 mm and extended a few mm into the cavity. In order that neither air nor helium could enter, this section of the waveguide was isolated from the rest of the microwave system and made vacuum tight by the two Teflon gaskets. The gas inlet tube was sealed into the short waveguide section with red sealing wax.

Low Temperature Apparatus.* A conventional duck billed double dewar system, shown disassembled in figure 5, held the liquid helium used as coolant in these experiments. The duck bill section was provided so that a rela-

---

*Figure 6 is a photograph of the assembled low temperature system.

tively small magnet gap(2-1/4") could be used. The dewars were suspended from a brass collar which in turn was hung from the ceiling by four nylon cords. This collar also served as a seat for arm 3 of the microwave bridge. Two copper pipe fittings projected from the collar in the form of a T. The larger pipe was connected to a high capacity Kinney pump with which the inner dewar was evacuated prior to precooling.* The smaller pipe was connected to a one way mercury valve which allowed helium gas to escape and prevented air from entering the system. Helium was liquified in the Cryogenics Laboratory with a Collins helium cryostat and stored in conventional double dewar storage vessels. Helium was transferred from the storage vessels to the inner dewar by means of a vacuum jacketed transfer tube. Arm 3 of the microwave bridge passed through a brass cup which fitted over the dewar collar and was sealed with an O ring. A 3/4" hole at one side of the cap accommodated the transfer tube.

One of the unusual features of this set-up was that although a length of 3 cm brass waveguide whose upper end was at room temperature, was immersed in liquid helium the rate of helium evaporation was less than 200 cc/hr. The reason for this was that the waveguide possessed a large surface to volume ratio; thus, it was cooled very

---

* See experimental procedure section.

efficiently by the effluent helium gas rushing by it. Therefore, most of the heat coming down the waveguidewas absorbed in heating the effluent gas rather than in boiling the liquid helium.

EPR Spectrograph. A greatly modified version of the spectrograph built by Humphrey (7) was used to observe the EPR resonance of the free radicals. A fairly detailed description is given below of those parts which have been changed or were not included in his instruments.* The more fundamental concepts involved in the design of an EPR spectrograph will not be dealt with as they are fully described by Wertz (3), Bleany and Stevens (2), and Ingram (5).

A block diagram of the complete instrument (fig. 8) consists of four main divisions: 1) Magnet, 2) Magnetic Field Controller (referred to as the controller), 3) Microwave System, 4) Signal Detection System. Descriptions of these divisions follow.

1. Magnet. An A. D. Little Electromagnet of the type designed by Bitter (8) provided the magnetic field for the spectrograph. Polefaces machined for this experiment were cylindrical, 11" in diameter and made of Armco iron. The magnet air gap was 2-1/4". The magnet is shown open

*For a fuller description of those parts which are identical or have minor modifications, the reader is referred to Humphrey's thesis.

in figure 6 with the dewars hanging in place. Using these pole faces it was possible to attain fields as high as 1.9 weber/m^2 (1 weber/m^2 = 10^4 gauss). Since this magnet was of the high current low voltage type (an internal resistance of 0.5 ohms), it was originally planned to energize it by means of a 25KW DC generator whose field current was regulated to provide the necessary time stability of the field. This proved to be very difficult for electronic reasons and subsequently, it was found that three automobile storage batteries continuously charged through a water cooled 2.9 ohm buffer resistor would provide a reasonably steady current of 25 A. Residual fluctuations in the field were easily compensated by the controller.

Measurement and control of the magnetic field required three auxiliary coils. The modulation coil was a 610 turn coil of 22 gauge enameled copper wire wound on a bakelite form producing a modulation of 0 to 1.3 milliweber/m^2. The correction coil contained 2100 turns of 28 gauge enameled copper wire and could produce corrections of $\pm$ 2.0 milliweber/m^2 in the magnetic field. A pair of 2400 turn sweep coils were imbedded in the magnet yoke and provided wide sweeps of $\pm$ 0.03/weber/m^2.

2. Magnetic Field Controller.* The maintenance of a steady magnetic field of known strength is essential in any magnetic resonance spectrograph. Rough field stabilization was achieved by the use of storage batteries as a current source for the magnet. Precise stabilization was gained by the servo loop consisting of proton fluxmeter, phase sensitive detector A and DC power amplifier. The proton fluxmeter measured the B field in the magnet gap and any change therein was sensed by the phase sensitive detector. This detector supplied the DC power amplifier with a voltage whose size and polarity indicated the rate and direction respectively of the field drift. The power amplifier, actuated by this DC signal, supplied current to the correction coil in the magnet in such a way as to cancel the drift. Any drifts which were so large that the DC amplifier was driven into a nonlinear region actuated the field control relays thereby increasing or decreasing the output of the variable power supply to the two sweep coils. The auxiliary equipment in this section of the spectrograph will be considered in the more detailed description below.

---

*Shown in figure 7.

a. Proton Fluxmeter.* The probe or sensing element of this unit was a 2 cm bulb of 7 mm pyrex tubing filled with a 0.1 M $Fe(NO_3)_3 \cdot 6\ H_2O$ solution around which was wound a coil that together with a 250 $\mu\mu$fd precision variable capacitor formed an RF tank circuit. This tank circuit was connected to the 6J6 oscillator tube acting as a regenerative feedback amplifier or negative resistance. When the negative resistance cancelled the parallel resistance of the tank circuit, oscillations built up. A 6AK5 pentode amplified the RF voltage and applied it to one half of a 6AL5 diode detector. Rectified RF current charged the 0.01 μfd capacitor so that a voltage of the form

$$V = A + Bf(t) \qquad (1)$$

appeared across the 20K fine level potentiometer. The first term represented the average level of RF oscillation and the second term any amplitude modulation of the RF. By means of the potentiometer, a portion of this voltage, after suitable filtering, was applied to the second grid of the 6J6. If the level of oscillation tended to rise, the increasing negative grid bias acted to keep

---

*A schematic diagram is shown in figure 9 and is labelled A in figure 7.

the gain of the second triode down, thus the level of oscillation was maintained at a low and constant level. Oscillation could be initiated by the 1K coarse level control. This circuit was a somewhat modified version of that published by Pound (9). When the resonance condition,

$$B_o = \omega_f / \gamma_p$$

where ω_f is the angular frequency of the fluxmeter and γ_p is the proton magnetogyric ratio, was fulfilled, the protons in the probe absorbed energy from the tank coil and caused an amplitude modulation of the RF output. In order to make use of a phase sensitive detector, the modulation must be recurrent periodically. This was accomplished by the field modulation amplifier (fig. 15) a 25 W push pull amplifer of conventional design. Its 400 cps input was supplied by a General Radio electronic tuning fork. The amplifier was connected to the modulation coil. *Thus, the field B in the gap was*

$$B = B_o + B' \cos(2\pi \cdot 400\ t) \qquad (2)$$

where B' may be varied from 0 to 0.6 milliweber/m^2. When the field B_o was such that the fluxmeter frequency equalled the proton resonance frequency at

$$\cos(2\pi \cdot 400\ t) = 0 \qquad (3)$$

and therefore

$$B_o = \omega_f/\gamma_p \qquad (4)$$

the RF output was modulated at 800 cps. If B_o had any other value in the range $\omega_f/\gamma_p \pm B'$, the modulation would have been 400 cps either in phase or 180° out of phase with the field modulation. Percentage modulation of the carrier was determined by the distance of the resonance field from the center of modulation.

The magnetic field was determined by measuring ω_f (the fluxmeter frequency) and substituting in equation 4 using

$$2\pi/\gamma_p = 2.34836 \times 10^{-8} \ \frac{\text{weber sec}}{m^2}$$

Frequency determination was made by obtaining a zero beat with the BC 221 N frequency meter (B in fig. 7). The zero beat was observed with a CRO (C in fig. 7) which also served to monitor the proton resonance line. A Haydon clock motor was attached to the tuning capacitor so that the fluxmeter frequency and thereby the field could be scanned slowly.

b. Phase Sensitive Detector A (7). A basic principle of a phase sensitive detector is that if two sinusoidal voltages are multiplied

together and the product integrated over a time long compared to the period of oscillation, it is found that there is no net voltage except when the two frequencies are identical and in this case there is a constant term proportional to Cos (d) where d is the phase difference between the two voltages. In a general case the voltages may be a Fourier series forming a complex waveform with the above principle applying to each of the terms of the Fourier series. Proof of these statements may be found in the book by Andrew (10).

Information in the envelope of the RF, i.e. the frequency and phase of its amplitude modulation, allowed the phase sensitive detector A to sense and correct the fluctuations in the magnetic field. The rather weak proton absorption signal was amplified by the first two stages of the detector. The two 6SL7's in this unit served as the actual detectors. The reference signal from the tuning fork was applied to the screen grids and the signal voltage to the signal grids. For a pentode the plate signal voltage E_p was

$$E_p = \mu_1 e_{g1} \mu_2 e_{g2}$$

where μ_1 and μ_2 are the amplifying factors and

e_{g1} and e_{g2} are the grid voltages. This fulfilled the condition for multiplication of the voltages. Following these tubes, there was an RC integrating circuit and a one stage difference amplifier.

c. DC Power Amplifier (7). This unit contained a pair of 6SL7's as another difference amplifier and a pair of 211's wired as cathode followers to supply current to the correction coil. One minor change was made in Humphrey's original circuit. The antihunt control was changed to a simple low pass RC filter in the grid circuit of the 6SL7's. Field control relays were identical to those described by Humphrey and were actuated by the voltage across the correction coil. In the present spectrometer, however, they controlled a DC motor which changed the setting of a variable autotransformer (Powerstat) in the variable power supply (fig. 11). Current for the 211's was supplied by the 1000 volt power supply (fig. 12) which was a full wave rectifier using 866 mercury vapor rectifier tubes and an inductance input filter. A 25v DC potential was also provided by a selenium rectifier half wave voltage doubler for the DC motor in the variable power supply. To prevent the high voltage being turned on until the filaments of the 866's were hot, a time delay switch was included.

3. Microwave Apparatus.* A war surplus radar test set (TS 13/AP) served as the radiation source providing up to 25 milliwatts of microwave power at frequencies of 8500-9600 mc. The circuit diagram (fig. 14) shows that the set consisted of two regulated power supplies, a 2K25 (723/AB) klystron and associated wave guides and attenuators. The original set included circuits for sawtooth and square-wave modulation which were disconnected. A thermistor bridge network and cavity wave-meter were also included but since these were not used in these experiments, they are not shown. The power supply using the 6AC7 and 6Y6G generates -300 V and was connected to the emitter of the 2K25. The other supply connected to the 2K25 reflector generated -210 V and was in series with the 300 V supply thus making the reflector -510 V below ground. Coarse frequency adjustments were made with the 2K25 tuning screw, fine adjustment with the 25K Helipot.

Microwave power output was controlled by two attenuators in the TS13/AP. One attenuator marked output was not calibrated, therefore was generally left at zero attenuation while the other

---

*Figure 13 shows a schematic diagram of the microwave section of the spectrograph.

attenuator, calibrated in db, was used to regulate the output. Following the TS13/AP, a Uniline microwave isolator prevented power reflected from the rest of the system from reaching the klystron and affecting its frequency. Frequency measurements were made with the Sperry cavity wavemeter. The variable stub tuner was an impedance matching device allowing maximum power to be transferred to the "magic Tee."

The magic Tee functioned as a microwave bridge--its purpose being to balance out almost all of the power reflected from the cavity. If arms 2 and 3 (H arms) of a magic tee are terminated by identical impedances, the power entering arm 1 will be divided equally between them and none delivered to arm 4 (E arm). Unequal impedances in arms 2 and 3 will unbalance the bridge and power will be transmitted to arm 4. Arm 3 (fig. 3), the sample arm of the bridge, consisted of approximately 1 m of waveguide terminated by a rectangular reflection cavity operating in the TE_{011} mode which was coupled to the waveguide through a 4 mm iris. The iris also served as the inlet for the dissociated gas. Arm 2 contained a waveline precision attenuator and a movable shorting plunger. These

served as the real and imaginary parts respectively of a variable impedance that was used to match the impedance of the cavity. Arm 4 contained a tunable crystal mount in which was a 1N23 silicon crystal diode. Because of the low power level in arm 4, the crystal current was kept low, thus improving the signal to noise ratio. Full discussion of this point is given by Ingram (5).

Since both the sample cavity and microwave bridge had an extremely frequency sensitive response, it was vital to keep the klystron frequency constant to within one part in 10^5. A fair degree of stability was achieved by using regulated power supplies to power the klystron. Slight variations in the temperature of the klystron, however, changed its frequency so that even perfectly regulated power supplies would not have produced the desired stability. Instead, a feedback system was used to compensate for thermal and electrical drifts. This was the purpose of the 10KC oscillator (7) and the AFC (7) unit. As shown in circuit diagram (fig. 14), the 10KC oscillator output was applied to the repeller of the klystron in the TS13/AP--frequency modulating it sinusoidally

about an average frequency. One volt (pp) produced 0.13 mc modulation. The Q curve or frequency response, characteristic of the sample cavity, amplitude modulated the power entering arm 4 of the bridge. Thus the action of the Q curve was made similar to that of the proton line described in the Fluxmeter section. If the klystron drifted to one side of the curve, an amplitude modulation of $\sin(2\pi \cdot 10^4 t)$ occurred while on the other side the modulation had an envelope of $\sin(2\pi \cdot 10^4 t + \pi)$ with respect to the modulation voltage. The amplitude modulation was detected by the 1N23 crystal in arm 4 of the Tee, amplified by the AFC, and fed to a ring modulator of IN42 diodes which acted as a phase sensitive detector. Any net DC voltage was amplified by a difference amplifier and applied to the repeller of the klystron so that it cancelled the frequency drift.

4. Signal Detection System (7). Only minor changes were made in this section of the spectrograph. In the phase sensitive detector B these included conversion of the twin tee filter to 400 cps operation, removal of the variable twin tee filter and an increased resistance in series with the Brown recorder balancing potentiometer.

A 3000 mfd capacitor was placed in parallel with the mercury cells that biased the filtering capacitors. This change was necessitated because the internal resistance of the cells was 50 ohms; therefore, unless this resistance was bypassed no filtering took place at all. A further modification of the system was made by the addition of a chopper driver. As seen in the circuit diagram (fig. 10) this was a simple cathode follower using a 6AS7 power triode and designed to match the chopper impedance of 28 ohms. A phase shifting network was provided so that the phase sensitive detector could be adjusted for maximum output.

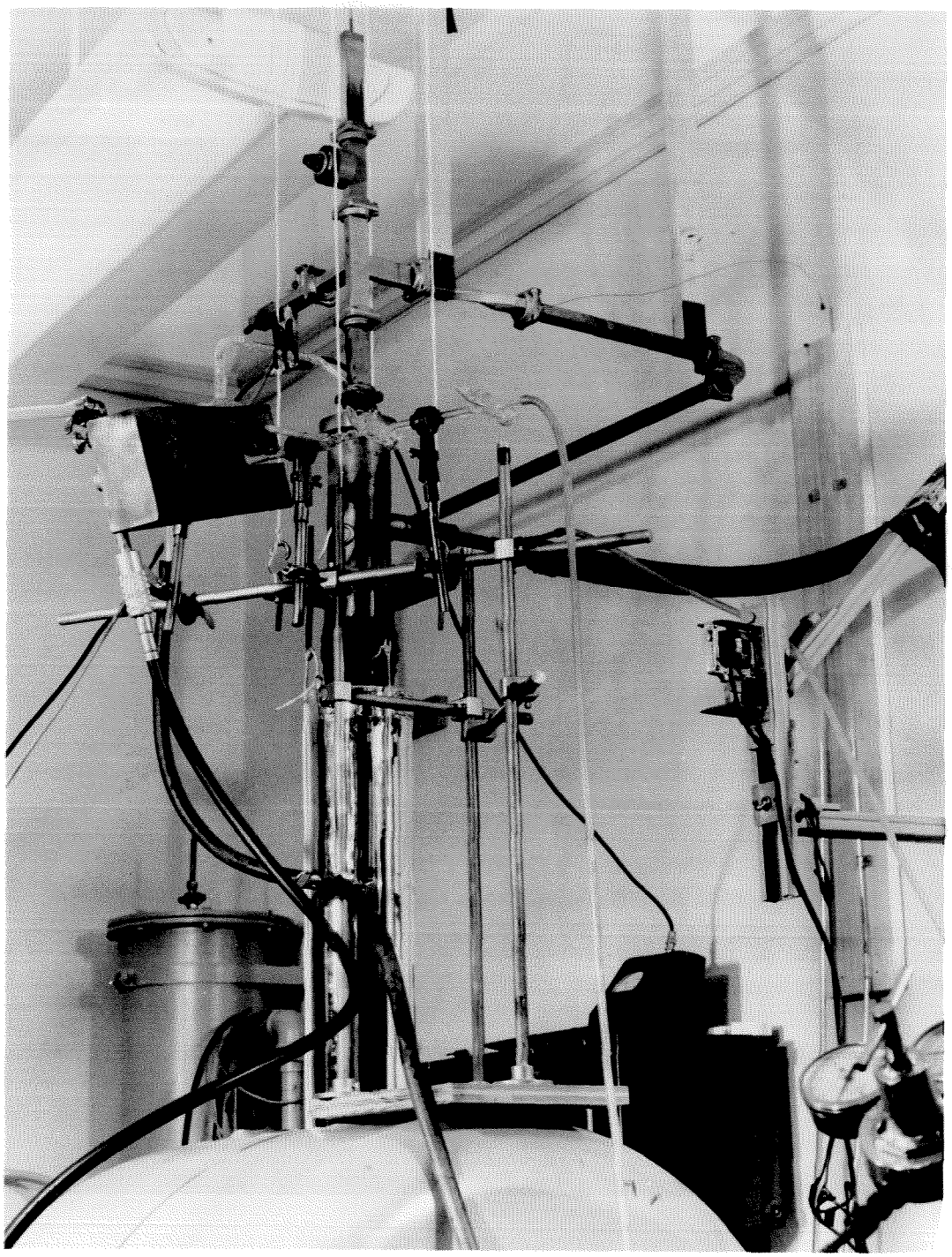

Fig. 1. Closeup showing gas dissociation apparatus.

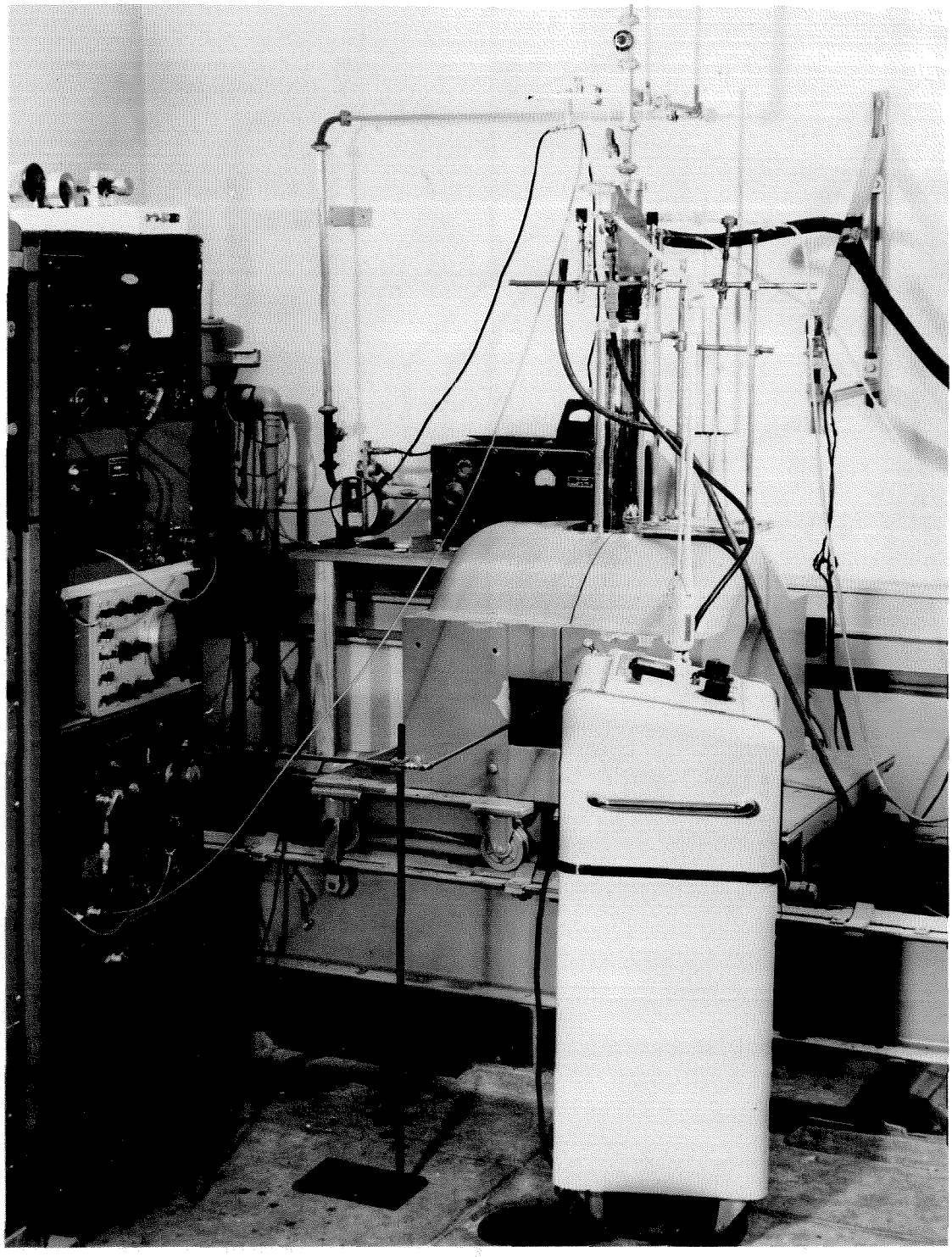

Fig. 2. Complete apparatus set up in preparation for an experiment.

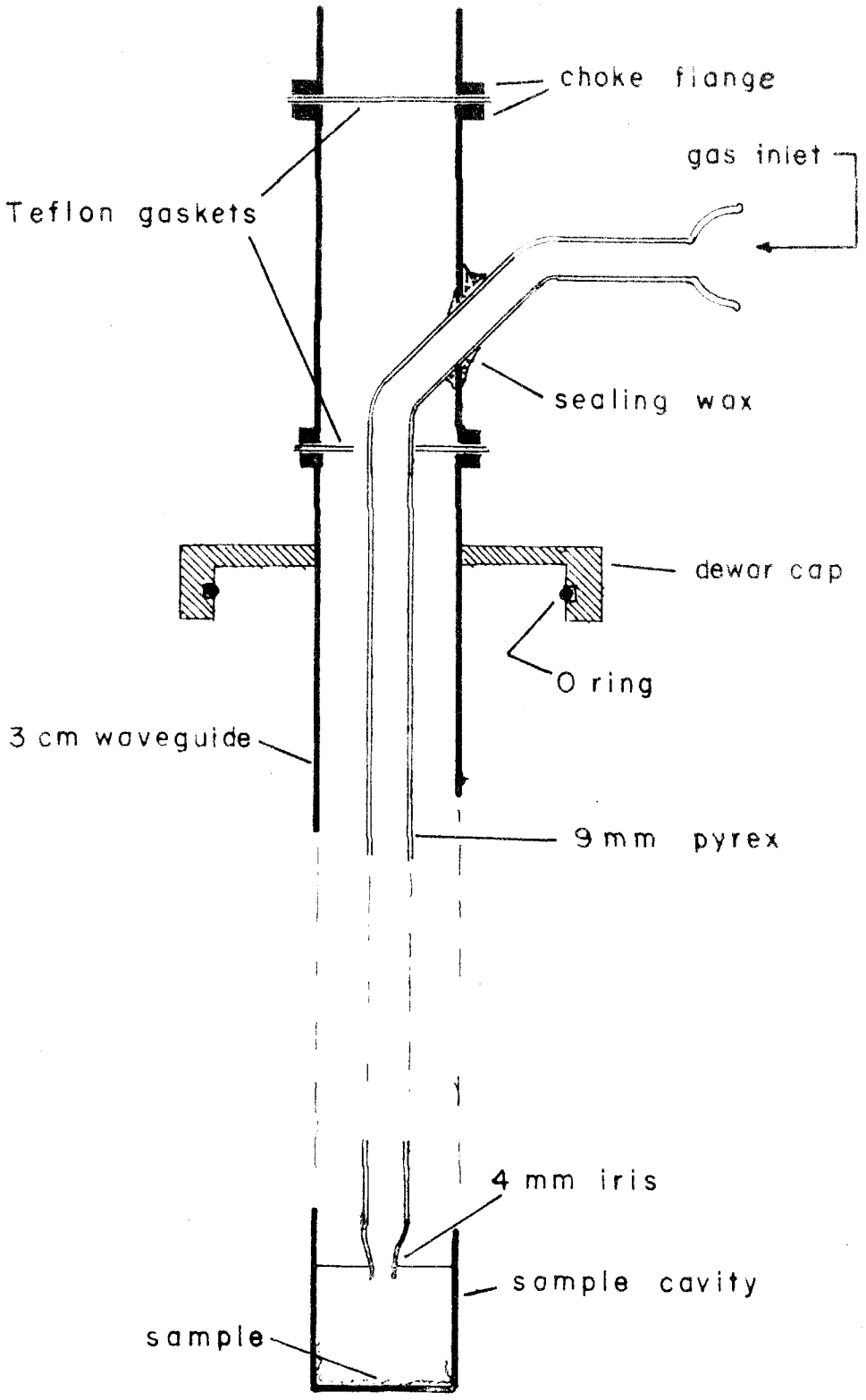

Fig. 3 Cutaway diagram of arm 3 of microwave bridge

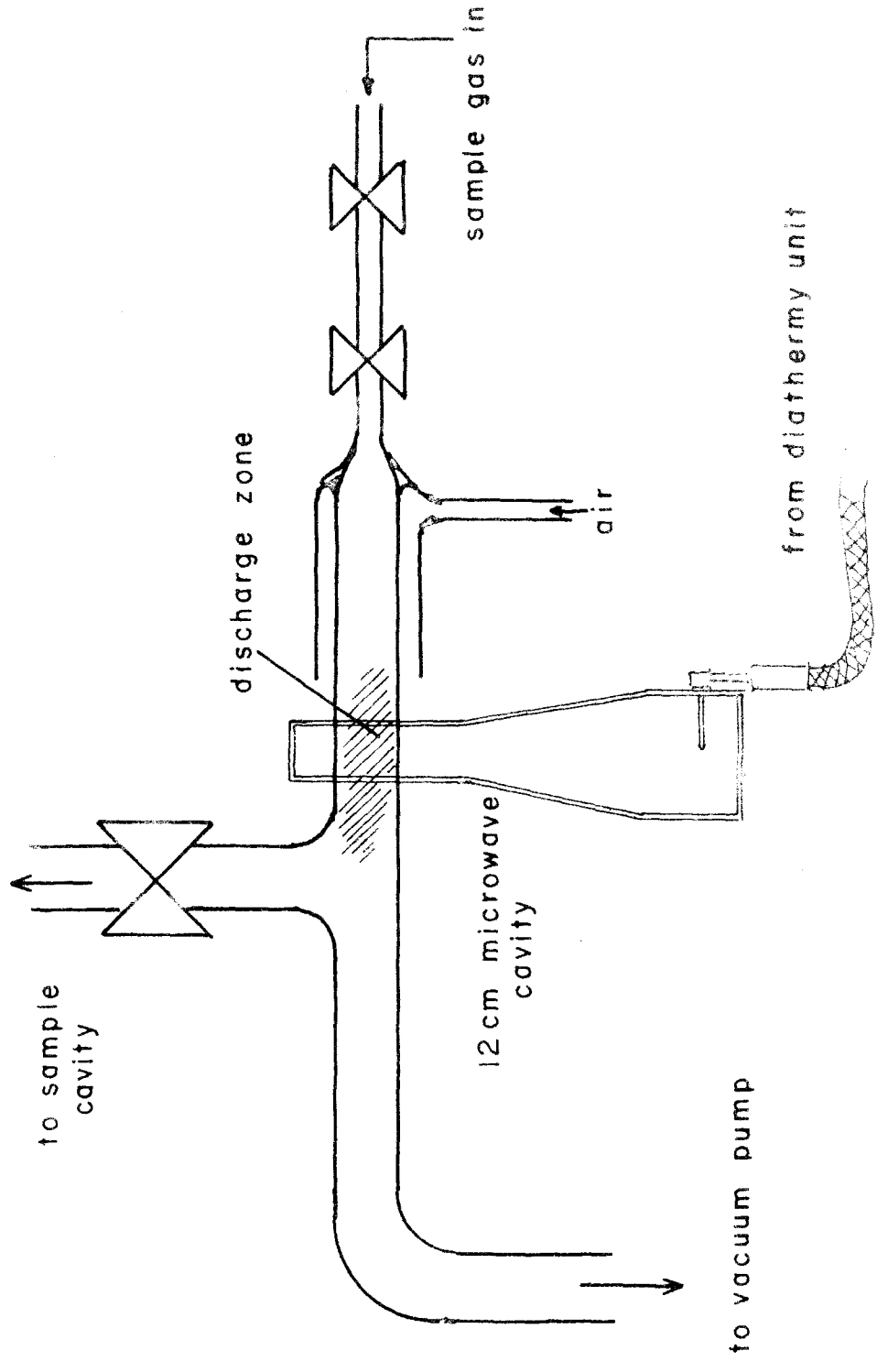

Fig. 4 Diagram of gas dissociation apparatus

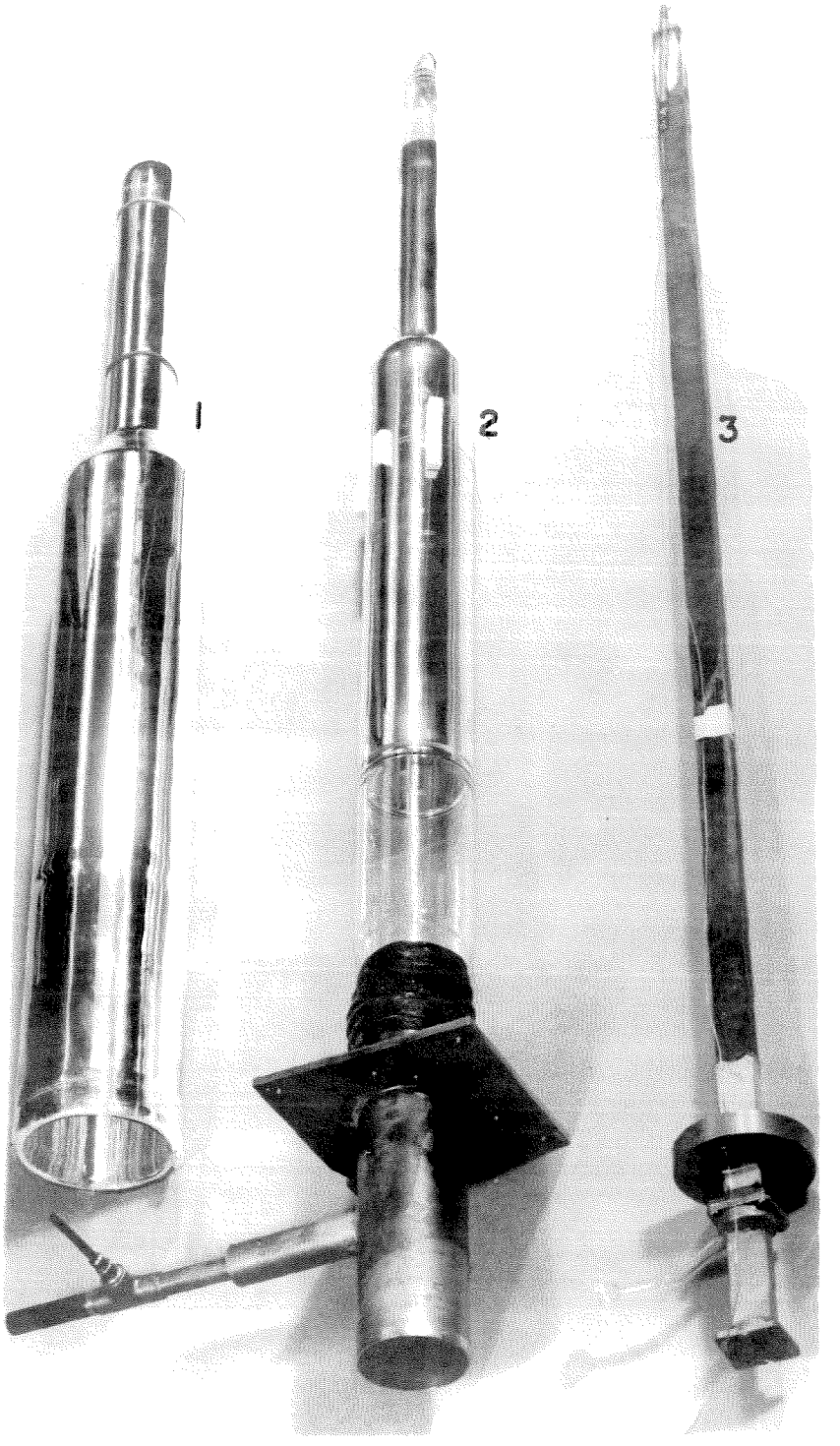

Fig. 5. Low temperature system disassembled showing 1 to 3 liquid N_2 dewar, liquid helium dewar, and arm 3 of microwave bridge.

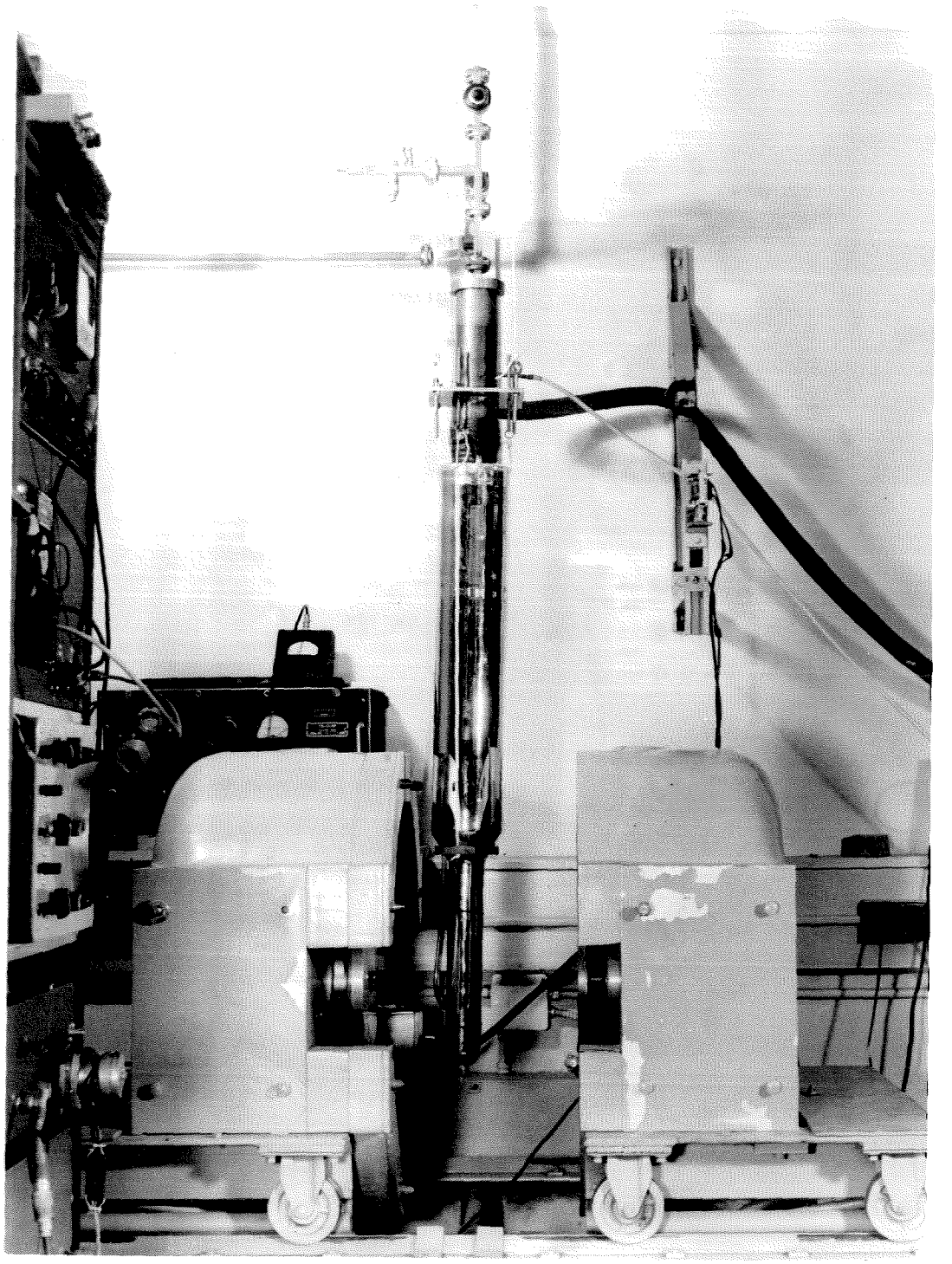

Fig. 6. Low temperature system between poles of magnet.

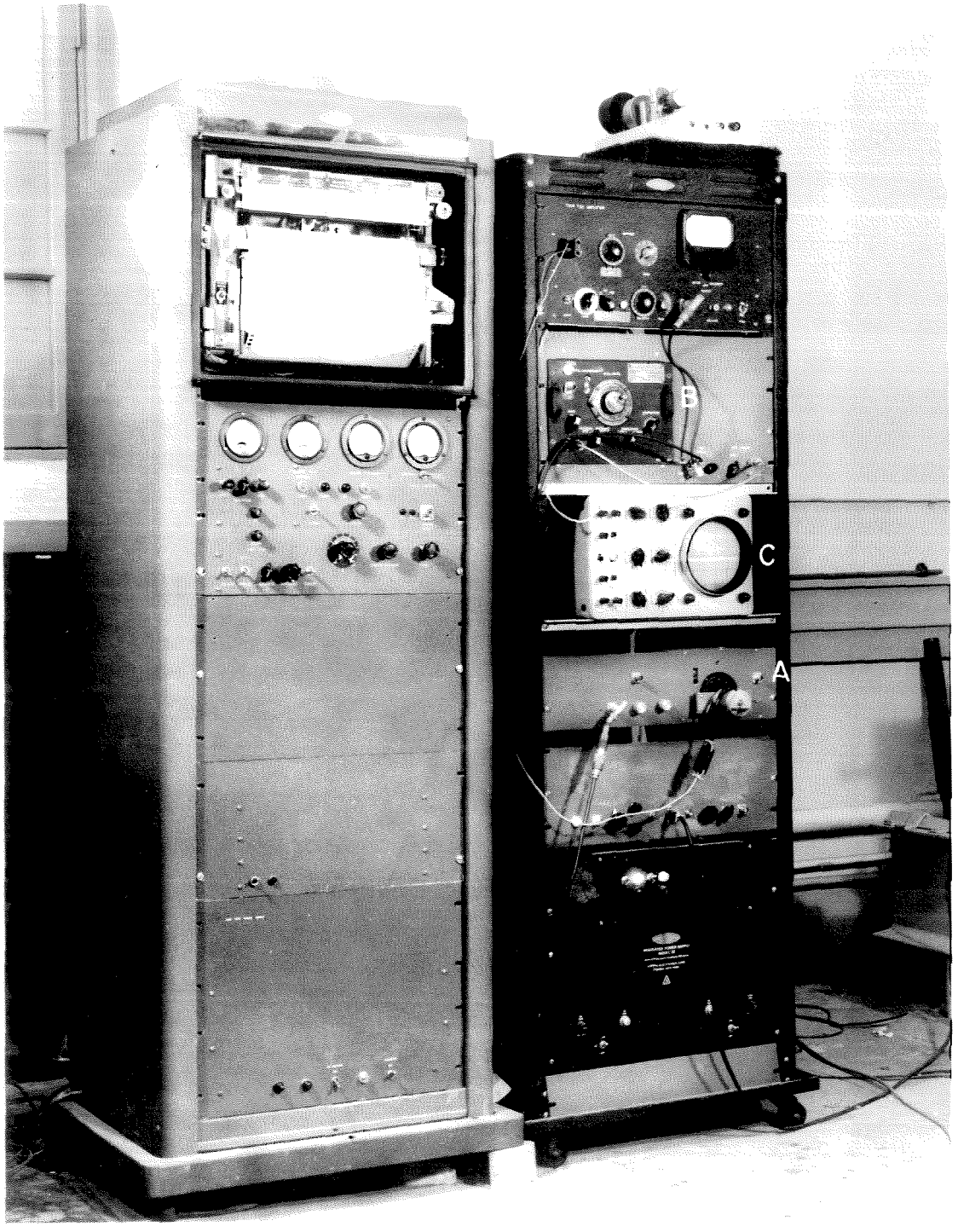

Fig. 7. Magnetic field controller.

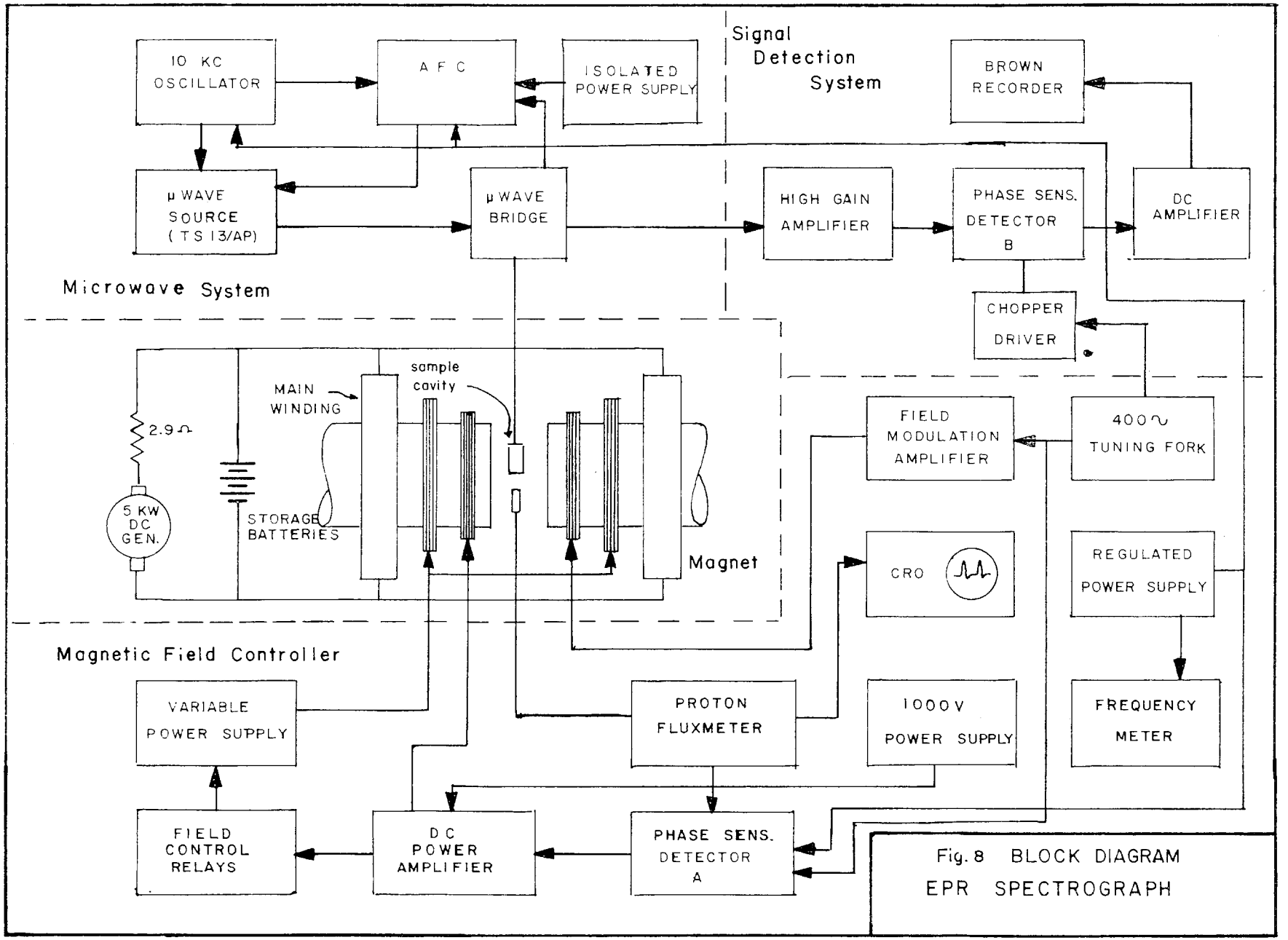

Fig. 8 BLOCK DIAGRAM
EPR SPECTROGRAPH

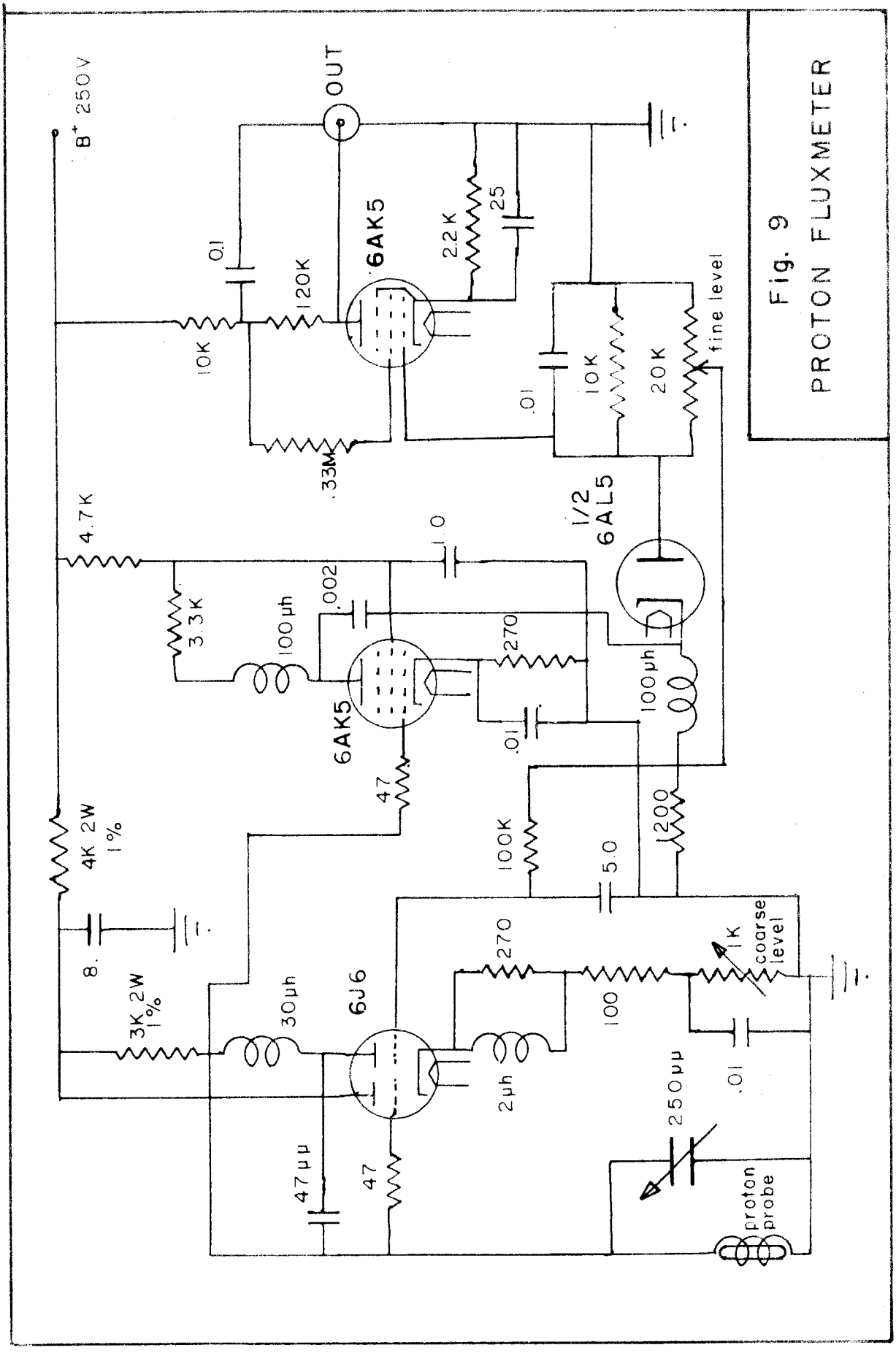

Fig. 9
PROTON FLUXMETER

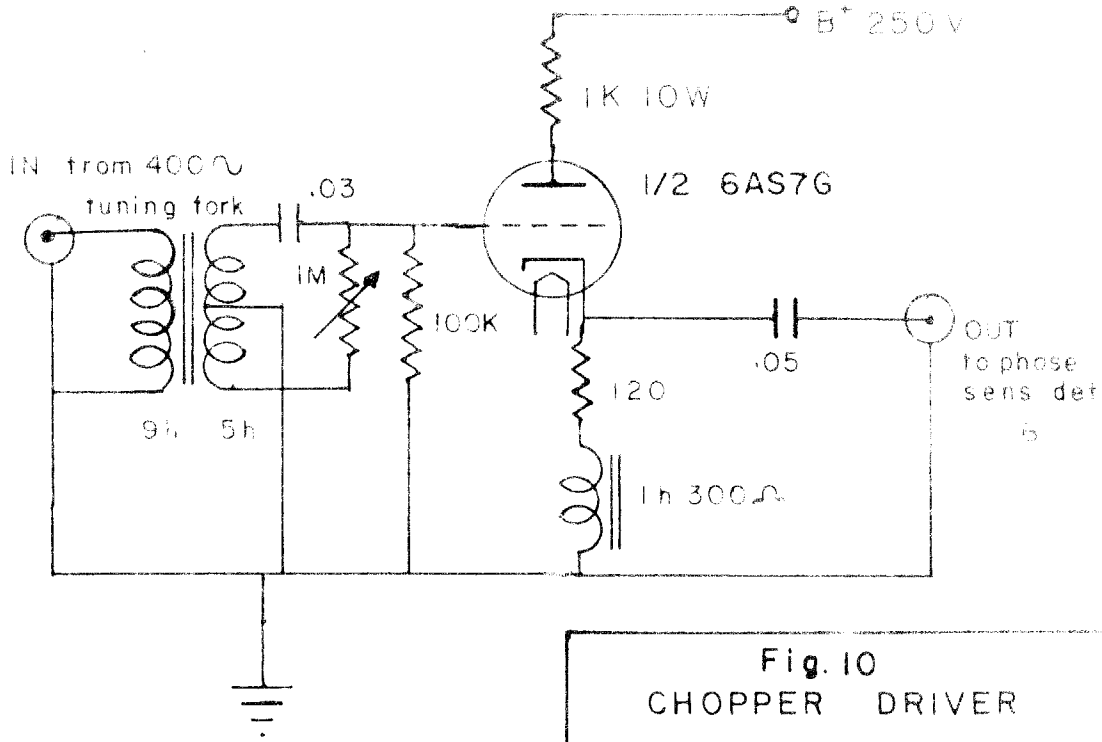

Fig. 10
CHOPPER DRIVER

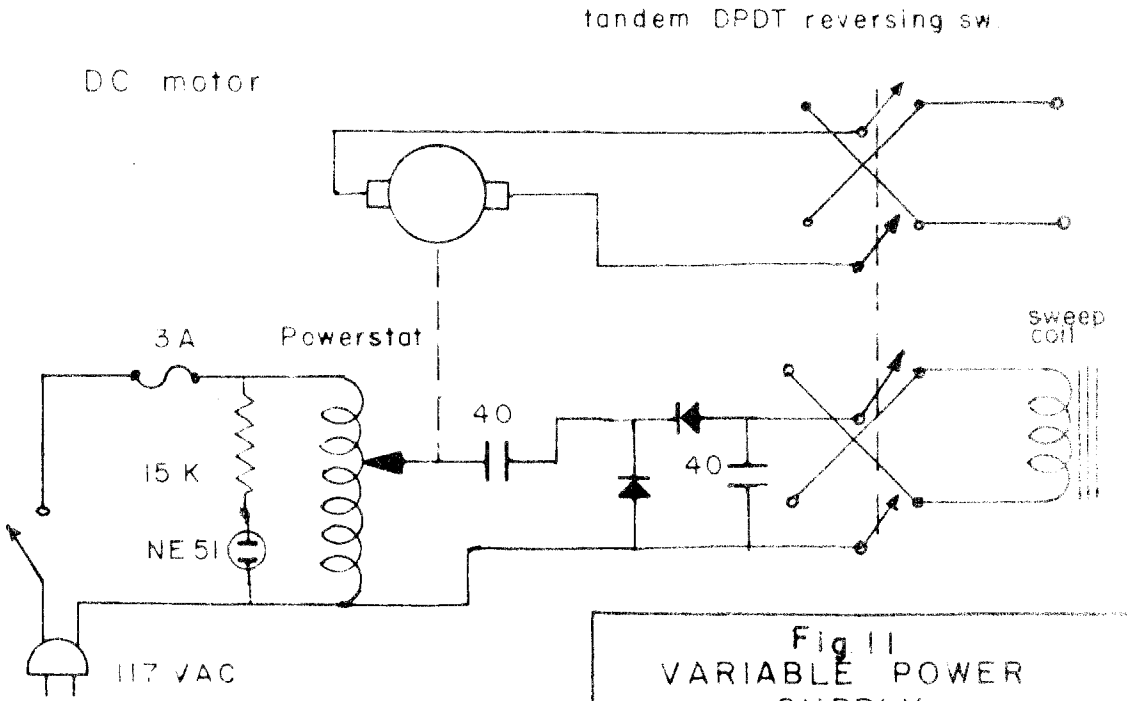

Fig. 11
VARIABLE POWER
SUPPLY

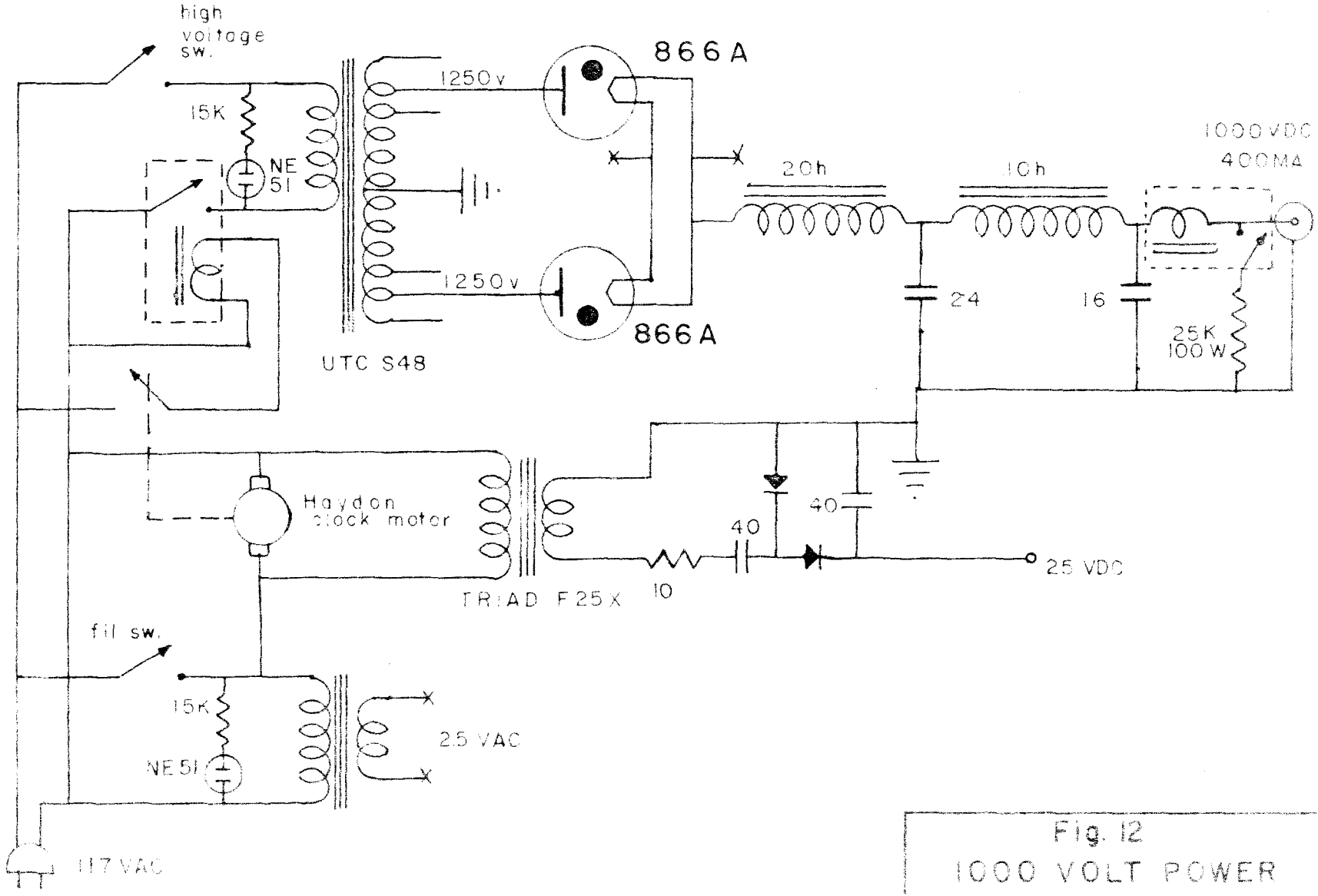

Fig. 12
1000 VOLT POWER SUPPLY

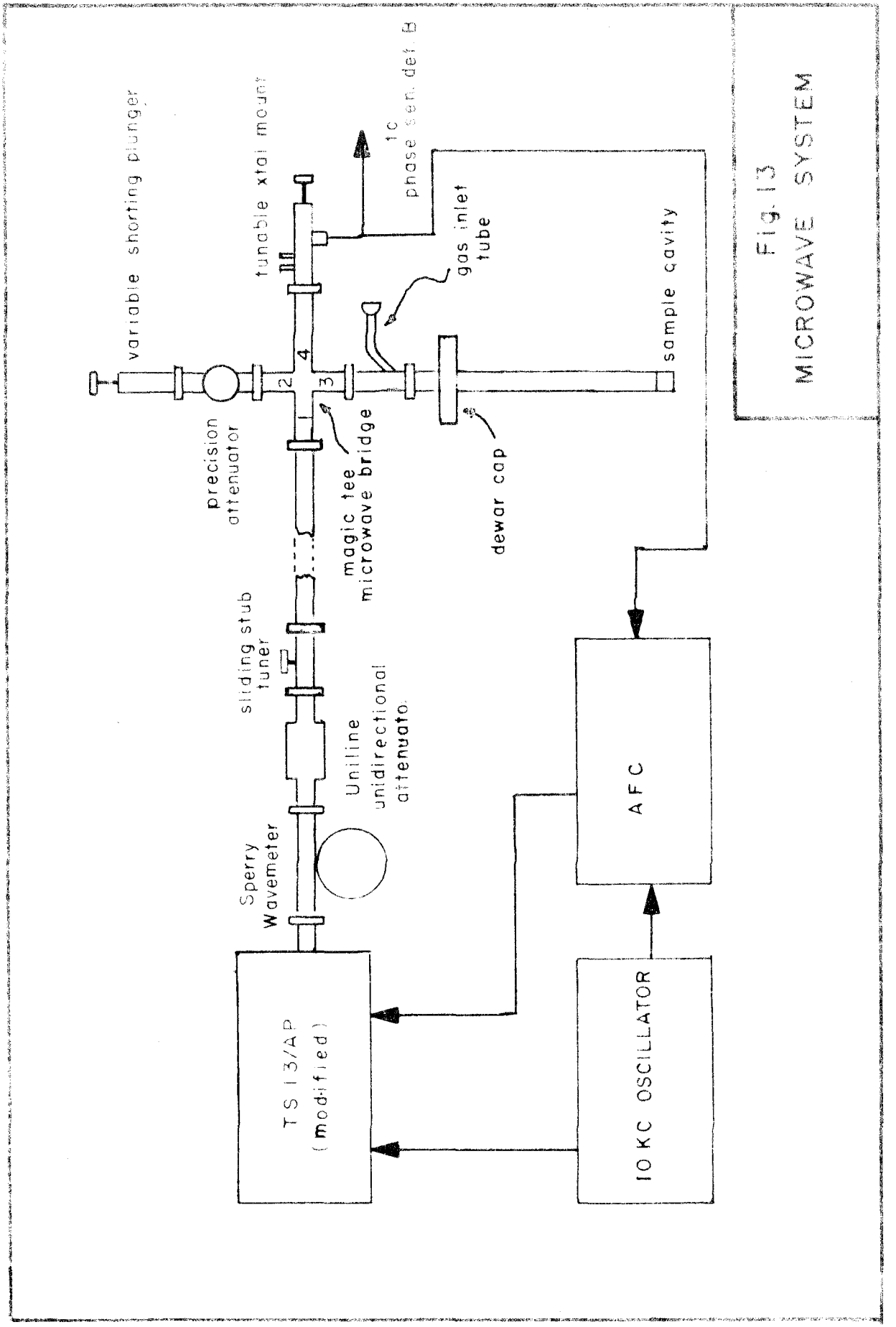

Fig. 13
MICROWAVE SYSTEM

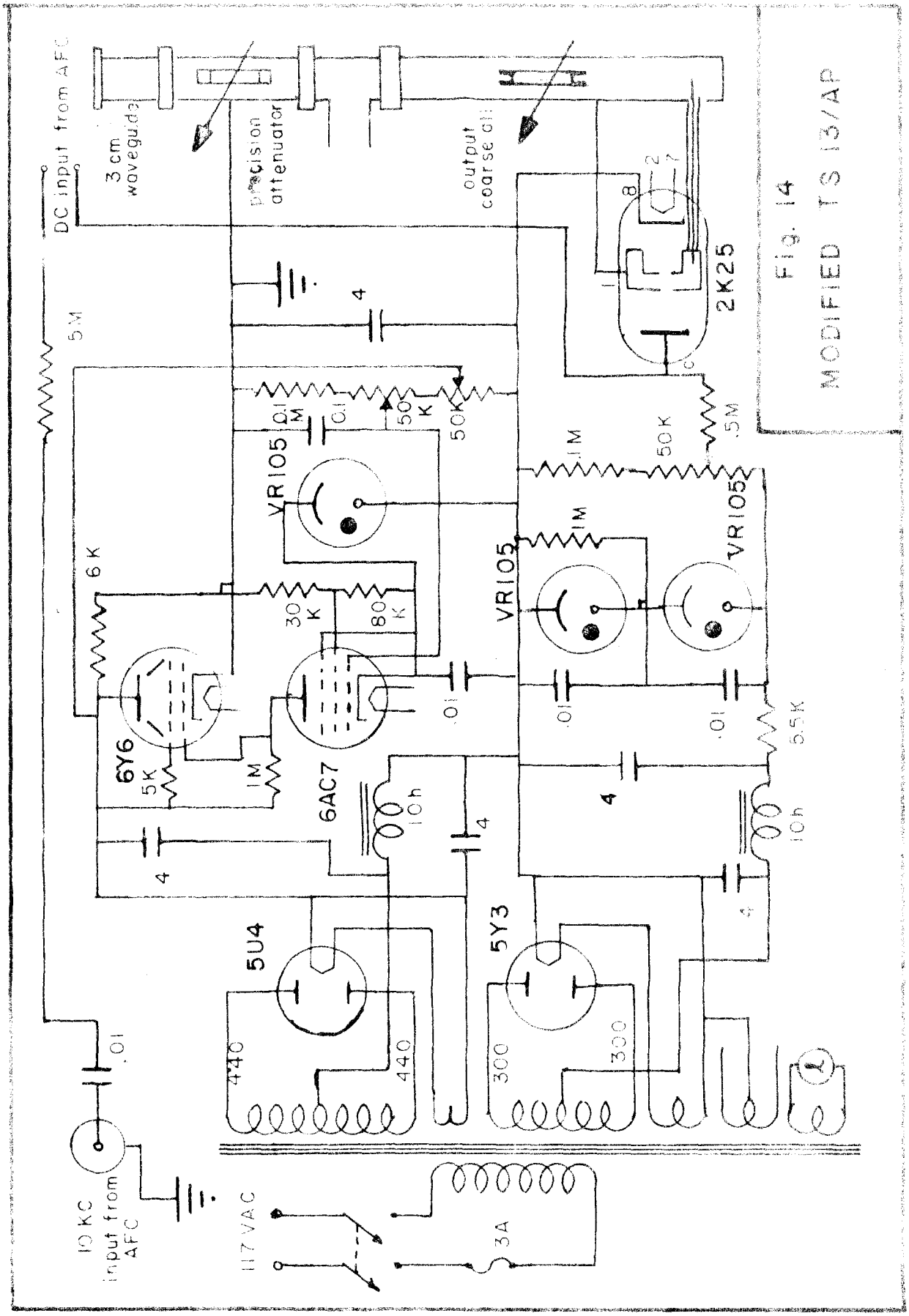

Fig. 14
MODIFIED TS 13/AP

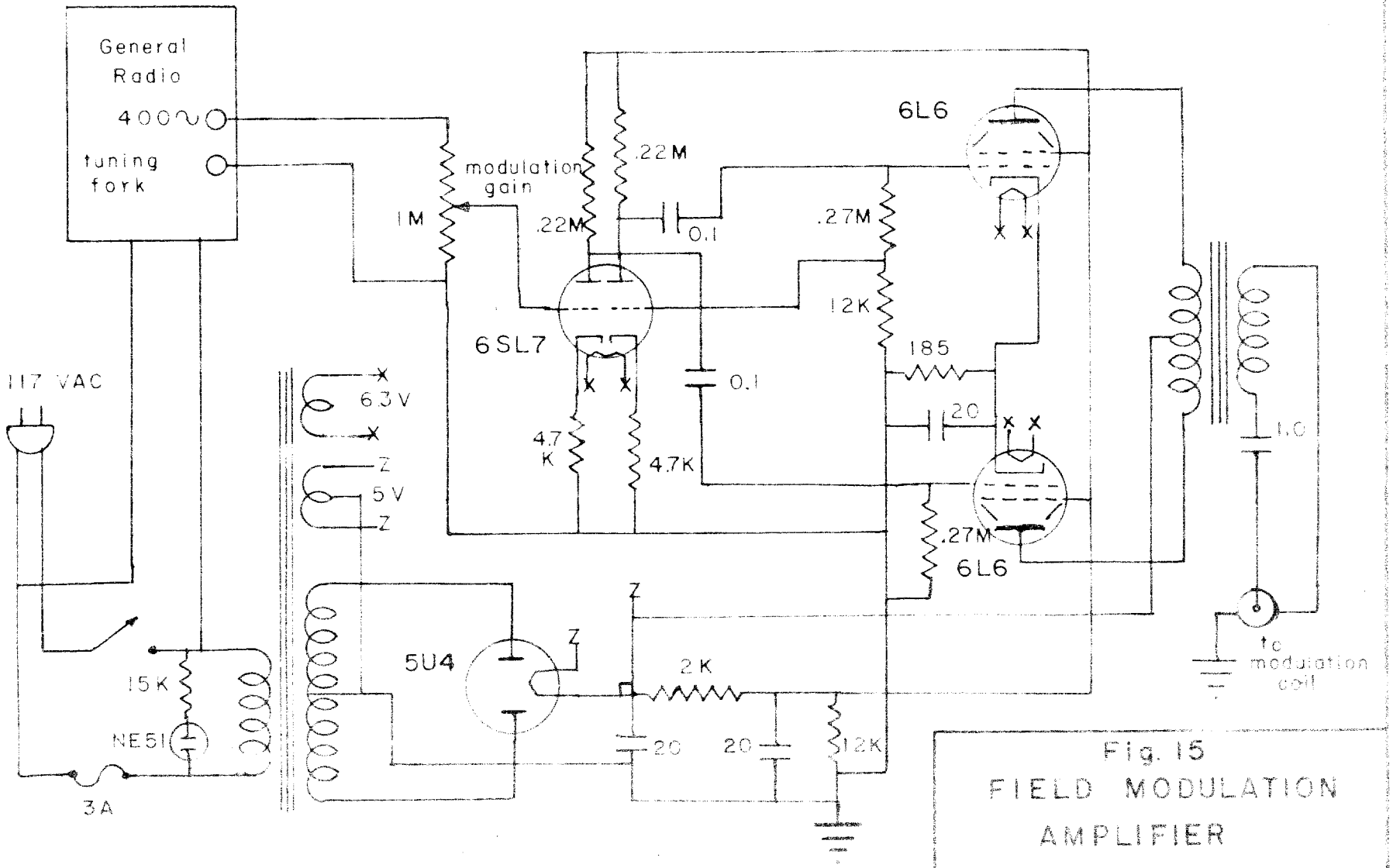

Fig. 15
FIELD MODULATION AMPLIFIER

EXPERIMENTAL PROCEDURE

Experiments on all of the substances followed the same schedule of operations:

1. Isolation. Subsequent to the assembly of the dewar system, sample arm of the bridge and gas system as described above, the inner dewar was evacuated with a high capacity Kinney pump to 0.1 mm Hg or less. The valve connecting the system to the pump was then closed and the pressure observed for several minutes to check for leaks. If no leaks occurred, the inner dewar was filled to a few mm above atmospheric pressure with dry helium. A one way Hg bubbler maintained this pressure thus preventing air from leaking back into the system.
2. Precooling. One and one-half hours before the helium was transferred, the inner dewar and sample cavity were precooled by filling the space between inner and outer dewar with liquid N_2.
3. Transfer. The inner dewar was filled from one of the storage dewars with approximately 3 liters of liquid helium. At this point the magnet was turned on and the field controller set on automatic.

4. Deposition of the Sample. Using the sawtooth sweep from a Cathode Ray Oscilliscope (CRO) to frequency modulate the klystron, the crystal output from arm 4 of the tee was displayed on the CRO. The tuning of the klystron was adjusted so as to display the cavity resonance curve. After placing the diathermy cavity over the discharge tube, the air cooling jet was turned on and the diathermy unit adjusted to approximately 80% full output. With the valve leading to the sample cavity closed, a small amount of sample gas was admitted to the discharge tube through the regulating stopcocks; the discharge was then started with a Tesla coil. The valve leading to the sample cavity was opened while observing the cavity Q curve on the CRO. Deposition was stopped when the Q curve had shifted approximately 20 mc and the Q had decreased 20%.

5. Microwave Adjustment. Sample cavity frequency was measured by tuning the Sperry wavemeter until its Q curve was superimposed on that of the cavity and the frequency read on the wavemeter scale. The wavemeter was then tuned approximately 100 mc away from the cavity frequency. To balance the tee, alternate adjustments were made of the attenuator and shorting plunger in arm 2 until

a monitor microammeter indicated approximately 5-10 microamperes crystal current with the klystron output at maximum and the Q curve appeared symmetrical on the CRO. Amplitude of the CRO sweep was decreased to zero while adjusting the klystron repeller voltage to keep the Q curve at the center of the trace. Klystron modulation was then disconnected from the CRO, and connected to the 10 kc output of the AFC which was switched to automatic.

6. Spectrum. The capacitor dial of the proton fluxmeter was turned manually until the magnetic field was near the expected electron resonance field. An appropriate sweep gear was chosen for the sweep motor which was then attached to the fluxmeter. The spectrum was run as described in the controller section.

NITROGEN

Lewis (11) in 1900 discovered that upon passing an electric discharge through a bottle containing N_2 at low pressure, a yellow glow was produced which persisted for several seconds after the discharge stopped. Shortly afterward Rayleigh began a systematic study of this phenomenon and in a series of masterful papers (12, 13, 14) from 1911-1913 described in detail nearly all of the features of this afterglow that are known today.

The following is a brief summary of the properties of nitrogen afterglow sometimes known as active nitrogen:

1. It emits light in 3 bands in the visible spectrum, viz. yellow (brightest), red and green (13). These are identified as coming from excited electronic states of nitrogen molecules. Light is emitted by the gas for as long as five hours (15).
2. No emission lines corresponding to the spectrum of atomic N are found (12, 13).
3. The glowing gas is extremely reactive and forms nitrides and azides with metals over which it flows. These reactions usually produce light which when analyzed, invariably contains the bright line spectrum associated with metallic atoms (12).
4. Upon heating of a portion of a tube carrying the afterglow, the glow is found to be extinguished

in the heated region only to reappear in a cooler section downstream (12).

5. Reactivity of the gas is maintained in the heated section (12).
6. The active portion of the gas accounts for 0.1-0.5% by weight of the total.
7. The gas is approximately 10^{-8} molar in electrons and contains no detectable positive ions (16).

At present the most widely accepted theory of active nitrogen is that of Mitra (17) who contends that the active species in the glow are nitrogen atoms in the ^4S ground state and ^2D and ^2P excited states. Transition from these to the ground state are strongly forbidden and therefore are not seen in the spectrum of the glow. This theory is supported by Heald and Beringer (18) who obtained the EPR spectrum of ground state nitrogen atoms in the afterglow and also by the mass spectrometric studies of Jackson and Schiff (19).

A new phase of this problem was opened by Pellam and Broida (20) in 1954 with their discovery of the brilliant green glow in the Lewis Rayleigh afterglow condensed at $4.2^{\circ}K$. Although the spectrum of this afterglow contains some molecular bands, its strongest features by far are two brilliant lines at 19100 and 17800 cm^{-1} corresponding to atomic transitions $^2D \rightarrow {}^4S$ and $2p^2 5d\ ^2D \rightarrow 2p^2 3p\ ^4D$. An hypothesis of Broida and co-workers in recent papers (6, 21) is that crystalline fields in the solid perturb the

energy levels of the atom and increase the probability of these transitions relative to the probability in the gas phase. Evidence for this explanation is that the lines are shifted slightly from their free atom values and additional splittings are found. Besides the excited molecules present, it has been inferred by Pimentel (22) from infra red spectra that the solid also contains N_3.

Results

Figure 16 shows a composite of several EPR spectra from pure nitrogen consisting of three distinct lines whose estimated center values are marked A, B, and C. The splittings from the center line of the triplet are $4.0 \pm 0.2 \times 10^{-4}$ weber/m^2. The value of g_j for the center line is $2.0013 \pm .0005$. Two weak satellite lines may also be noticed at points 1 and 2; their separations from B are 1.4 and 1.6 milliwebers respectively. There was no noticeable decrease in signal after 2 hours indicating a half life of at least 10 hr. for the nitrogen atoms in the solid. Upon warming of the sample cavity to $77^{\circ}K$, the spectrum disappeared.

Analysis

The identification of the spectrum as that of nitrogen atoms rests on three points:

1. The value of g_j indicates an atom in an S state.

2. In its ground state, very nearly $1s^2 2s^2 2p^3\ {}^4S_{3/2}$, atomic nitrogen has a total electronic spin of S-3/2 and a nuclear spin of I = 1. As the Hamiltonian for an atom in an S state in a magnetic field, take

$$\mathcal{H} = -\hbar[\gamma_s \mathbf{S} + \gamma_I \mathbf{I}]\cdot \mathbf{B}_0 + A\,\mathbf{I}\cdot\mathbf{S}\hbar^2 \qquad (5)$$

where γ_s and γ_I are the magnetogyric ratios of the electronic and nuclear systems respectively; S and I are the angular momentum operators for the electronic and nuclear systems; A is the hyperfine coupling constant. First order perturbations result in three allowed magnetic dipole transitions (see Appendix 1)

$$\begin{aligned} h\nu &= \hbar\gamma_s B_0 \\ &= \hbar\gamma_s B_0 \pm A\hbar^2 \end{aligned} \qquad (6)$$

which correspond to the three strong lines observed.

3. The magnitude of the triplet splitting gives $\frac{A\hbar}{\gamma_s} = 0.40$ milliweber/m^2 of $\frac{A\hbar}{2\pi} = 11.2$ mc, as compared with 10.45 mc found by Heald and Beringer (18) for nitrogen afterglow at room temperature.

Second order perturbation calculations (Appendix 1) leads to an additional splitting which, if unresolved, produces a shift of the center of gravity of the order $1/4\left(\frac{A^2\hbar^3}{\gamma_s B_0}\right)$. For the above value of A and a field of 0.33 weber/m^2 which was employed, this

shift is 1.5×10^{-7} w/m^2, far below our limit of resolution.

No satisfactory explanation is available for the two weak satellite lines since they may represent only part of a weak spectrum which is obscured by the strong triplet.

Additional Experiments

The change in the size of the triplet splitting between the gas and solid afterglow may be caused by the energy level broadening surmised by Broida et al. (6,21). This view is supported by the line widths which would not be expected at these low temperatures. In order to determine the effect of the matrix on the spacing and line width of the triplet, pure N_2 was diluted 10:1 with dry argon and subjected to the same discharge and condensation. Results of this experiment are shown in figure 17. The lines have maintained the same spacing but have broadened by a factor of 2 to 3. This result is at first sight rather unexpected since if the original line width were due to dipole or crystalline electric field broadening, the lines would be expected to narrow upon dilution in an inert diamagnetic lattice containing no ion pairs. Broadening may be explained by assuming the argon to form a dense closest packed structure into which the nitrogens are fitted as defects--their electron clouds and thereby their energy levels being perturbed by this crowding.

It may be suggested that a more open lattice should be chosen for the diluting matrix but here one is faced with the task of finding an open lattice sufficiently inert that it will not react with free nitrogen atoms. A possible solution is to dilute the afterglow downstream from the discharge zone with a quantity of undissociated nitrogen gas. By this procedure one could determine whether the broadening were a magnetic dipole-dipole effect or due to the quadrapole electric field of N_2.

During the course of one of the nitrogen experiments the complex spectrum shown in figure 18B was obtained. When the sample cavity was warmed to 77°K, the spectrum disappeared. Upon subsequent dismantling of the apparatus, it was found that several small droplets of mercury had been drawn into the discharge tube. Each of the droplets was surrounded by a green powdery deposit, the same deposit being found on the walls of the sample cavity. The spectrum obtained contains 11 lines of varying intensity ranged unsymmetrically about a strong central line at $g_j = 2.0046 \pm .0005$. No explanation of these lines can be given at present.

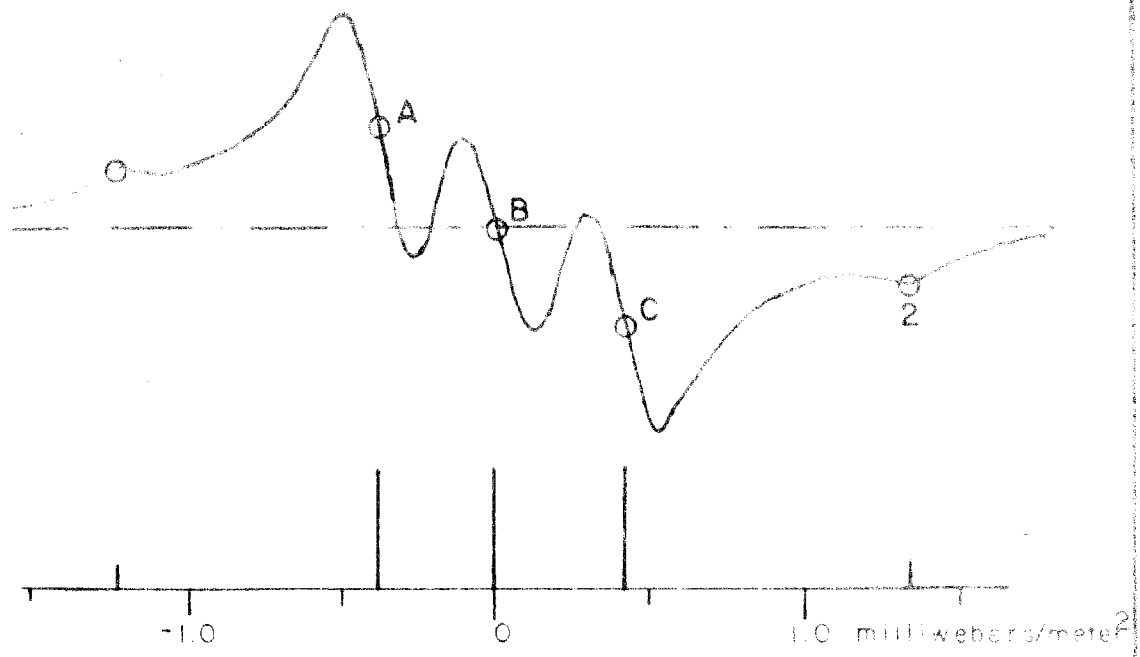

Fig. 16 EPR Spectrum of Nitrogen Atoms

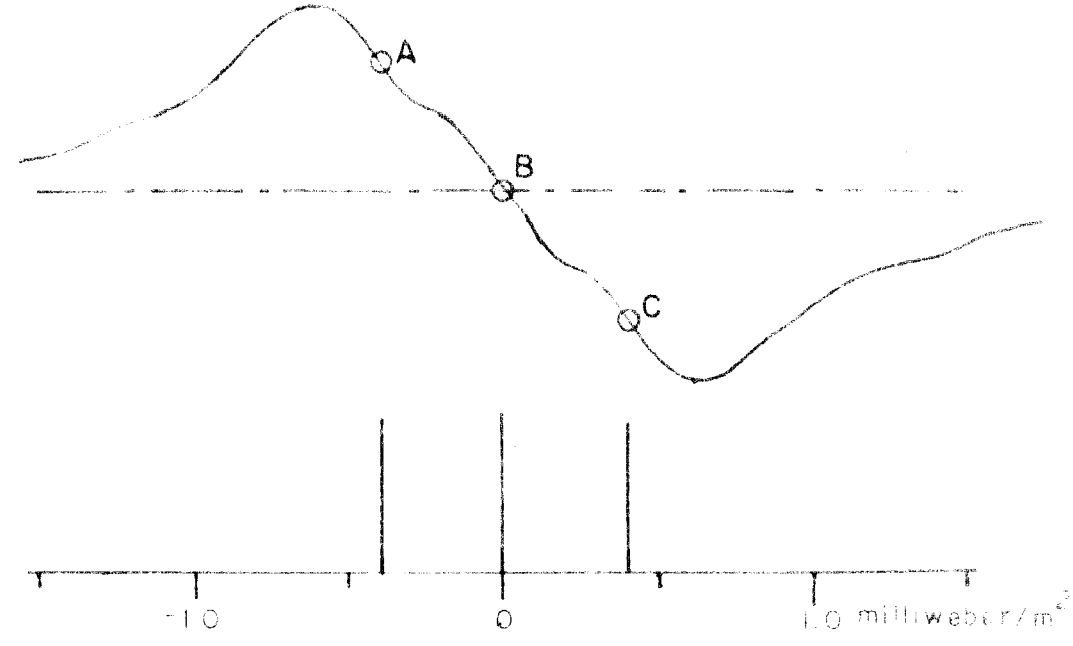

Fig. 17 EPR Spectrum of N Atoms Diluted with Argon

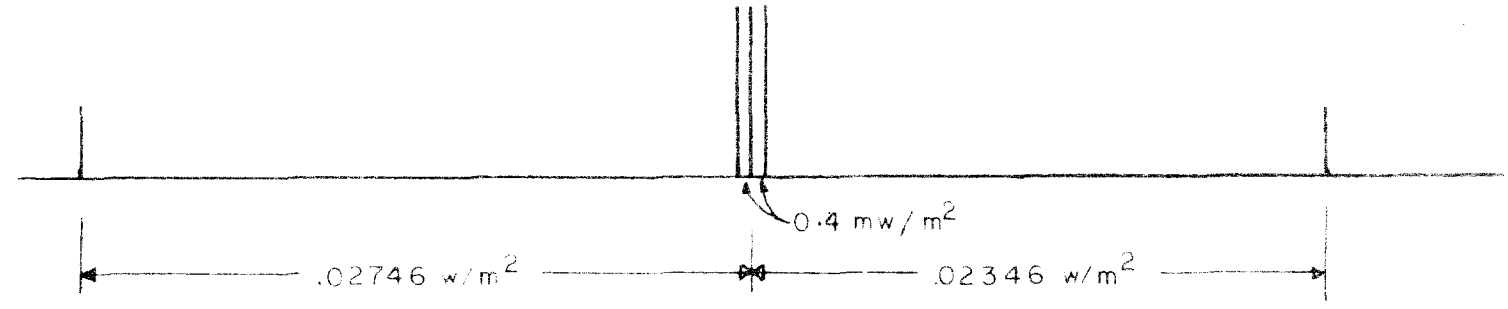

(A)

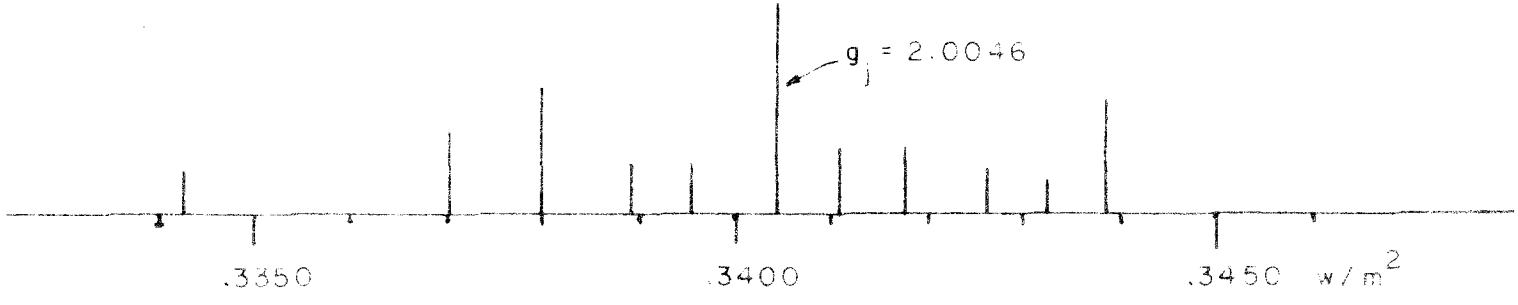

(B)

mw/m² = milliweber/meter²
w/m² = weber/ "

Fig. 18 EPR Spectrum of dissociation products of NH_3 (A) & Active Nitrogen Passed over Hg. (B)

AMMONIA

In order to test the general applicability of the techniques developed for N_2 to other compounds, it was decided to substitute NH_3 for N_2 in the dissociation apparatus.

Results

The discharge produced by the diathermy unit in the NH_3 was of a reddish color and was not followed by any afterglow. A composite of the EPR spectra (fig. 18A) consisted of a closely spaced triplet at g = 2.002 and a wide doublet unsymmetrical with respect to g = 2.0. The triplet splitting was symmetrical and equalled 0.4 milliweber/m^2. Total doublet splitting was 50.95 milliweber/m^2 and had a center 2.0 milliweber/m^2 below the field value for g_j = 2.00. The line widths were between 0.2-0.3 milliweber/m^2.

Analysis

The two portions of the spectra are interpreted as being the resonances of free hydrogen and nitrogen atoms--the former giving rise to the doublet and the latter, the triplet. The value of the splitting for nitrogen checks closely with that given in the nitrogen section above. The doublet splitting and center of gravity shift of 2 milliweber/m^2 correspond to the values found for H atoms trapped in H_2 by Jen and Foner (23). It also is in agreement with the well known 1420 mc splitting of the ground state of hydrogen (24).

The wide satellites found in N but not in NH_3 discharge products should also be noted. There is no evidence in these spectra of the presence of NH or NH_2. This, however, does not preclude their presence in the sample. NH, being in a $^3\Sigma$ state, may have zero field splitting between the 3 spin levels. This splitting may be large compared with $h\nu$ for the microwave radiation so that no resonance could be observed. In the case of NH_2 the odd p electron possesses orbital angular momentum which may or may not be quenched by the intramolecular electric fields. If the angular momentum were quenched leaving spin-only angular momentum, one would expect to find a set of hyperfine multiplets around g = 2.00. If the orbital momentum was not quenched, the EPR lines of this electron would be far outside the region of fields investigated and could be so broadened that they would be undetectable.

Theoretical calculation of the size of these splittings for both NH and NH_2 is a problem of practically insuperable difficulty. It is therefore possible that a spectrum from either or both of these might be present but be completely masked by the strong N triplet observed. It is interesting to note that Rice and Fremano (25) have found no evidence for NH in the discharge products of NH_3 frozen at liquid N_2 temperatures.

REFERENCES

1. K. K. Darrow, Bell. Sys. Tech. J., 32, 74 (1953).
2. B. Bleaney and K. W. H. Stevens, Repts. Progr. in Phys., 16, 108-159 (1953).
3. J. E. Wertz, Chem. Rev., 55, 829-955 (1955).
4. W. Gordy, W. V. Smith and R. F. Tambaralo, "Microwave Spectroscopy," John Wiley and Sons, New York (1953).
5. D. J. E. Ingram, "Spectroscopy at Radio and Microwave Frequencies," Butterworth, London (1955).
6. A. M. Bass and H. P. Broida, Phys. Rev., 101, 1740-1747 (1956).
7. F. B. Humphrey, "Ph.D Thesis," C.I.T., 1956.
8. F. Bitter and F. E. Reed, Rev. Sci. Instr., 22, 171-173 (1951).
9. R. V. Pound, Progr. in Nuc. Phys., 2, 21-50 (1952).
10. E. P. Andrew, "Nuclear Magnetic Resonance," Cambridge Univ. Press (1955), p. 44.
11. P. Lewis, Ann. d. Phys., 2, 466 (1900).
12. Lord Rayleigh (R. J. Strutt), Proc. Ray. Soc., A85, 219-219 (1911).
13. A. Fowler and R. J. Strutt, ibid., A85, 377-388 (1911).
14. Rayleigh, ibid., A88, 539-549 (1913).
15. Rayleigh, ibid., A151, 567-584 (1935).
16. J. Benson, J. App. Phys., 23, 757-763 (1952).
17. S. K. Mitra, Phys. Rev., 90, 516-521 (1953).

18. M. Heald and R. Beringer, Phys. Rev., 96, 645 (1954).

19. D. S. Jackson and H. I. Schiff, J. Chem. Phys., 22, 33-34 (1953).

20. H. P. Broida and J. R. Pellam, Phys. Rev., 95, 845 (1954).

21. C. M. Herzfeld and H. P. Broida, Phys. Rev., 101, 606-611 (1956).

22. G. C. Pimentel, private communication.

23. C. K. Jen, S. N. Foner, E. L. Cochran and V. A. Bowers, Phys. Rev., 104, 846-847 (1956).

24. J. E. Nafe and E. B. Nelson, Phys. Rev., 73, 718 (1948).

25. R. O. Rice and M. Freamo, J.A.C.S., 75, 548-549 (1953).

APPENDIX

To calculate the energy levels for an atom in a magnetic field B_o with J = S = 3/2 and I = 1 we use the Hamiltonian,

$$\mathcal{H} = -\hbar(\gamma_s \mathbf{S} + \gamma_I \mathbf{I}) \cdot \mathbf{B}_o + A\hbar^2 \mathbf{I} \cdot \mathbf{S} \qquad (1)$$

γ_s = magnetogyric ratio of the electronic spin system

γ_I = magnetogyric ratio of the nuclear spin system

$\mathbf{S}$ = electronic spin operator

$\mathbf{I}$ = nuclear spin operator

A = hyperfine coupling constant

In the strong field case when I and S are decoupled by the magnetic field we may take the first term on the right of equation 1 as the unperturbed Hamiltonian and the second as the perturbation. The unperturbed eigenfunctions may be written, using Greek letters to denote electron spin and English letters for nuclear spin, as follows:

αa	βa	γa	δa
αb	βb	γb	δb
αc	βc	γc	δc

where α, β, γ and δ are electronic spin functions corresponding to m_s = 3/2, 1/2, -1/2 and -3/2 respectively and a, b, and c correspond to m_I = 1, 0, and -1. The Hamiltonian for the atom may be rewritten.

$$\mathcal{H} = -\hbar(\gamma_s \mathbf{S} + \gamma_I \mathbf{I})\cdot \mathbf{B} + A\hbar^2[I_z S_z + \tfrac{1}{2}(I_+ S_- + I_- S_+)] \quad (2)$$

or

$$\mathcal{H} = \mathcal{H}_0 + A\hbar^2 \mathcal{H}^{(1)} \quad (3)$$

$I_{\pm}$ and $S_{\pm}$ are the spin raising and lowering operators.

$$S_+ = (S_s + iS_y)$$
$$S_- = (S_x - iS_y)$$
$$I_+ = (I_x + iI_y)$$
$$I_- = (I_x - iI_y)$$

We may now calculate the energy levels using the second order perturbation formula:

$$E = H_{0_{nn}} + A\hbar^2 H^{(1)}_{nn} + A^2\hbar^4 \sum_m{}' \frac{H^{(1)}_{nm}\, H^{(1)}_{mn}}{H_{0_{nn}} - H_{0_{mm}}} \quad (4)$$

where $H_{0_{nn}}$ are the unperturbed energies and

$$H^{(1)}_{nm} = \int \psi^*_n \mathcal{H}^{(1)} \psi_m \, d\tau \quad (5)$$

The new energy levels are:

Level	Energy
α a	- 3/2 V - X + 3/2 Y
α b	- 3/2 V - 3/2 Z
α c	- 3/2 V + X - 3/2 Y - 3/2 Z
β a	- 1/2 V - X + 1/2 Y + 3/2 Z

β b	-	1/2 V					-	1/2 Z
β c	-	1/2 V	+	X	-	1/2 Y	-	3/2 Z
γ a		1/2 V	-	X	-	1/2 Y	+	3/2 Z
γ b		1/2 V					+	1/2 Z
γ c		1/2 V	+	X	+	1/2 Y	-	3/2 Z
δ a		3/2 V	-	X	-	1/2 Y	+	3/2 Z
δ b		3/2 V					+	3/2 Z
δ c		3/2 V	+	X	+	3/2 Y		

where

$$V = \hbar \gamma_s B_o$$

$$X = \hbar \gamma_I B_o$$

$$Y = A\hbar^2$$

$$Z = \frac{A^2\hbar^3}{\gamma_s B_o}$$

For nitrogen the Z terms are very small. From the selection rules $\Delta m_I = 0$, $\Delta m_S = \pm 1$ we obtain three lines at:

$$h\nu = \hbar \gamma_s B_o$$

$$= \hbar \gamma_s B_o + A\hbar^2$$

$$= \hbar \gamma_s B_o - A\hbar^2$$

PROPOSITIONS

1. Matheson and Smaller (1) have reported the EPR spectrum of gamma irradiated solid NH_3; it consists of 5 equally spaced lines covering a range of 7.7 milliweber/m^2. They have assigned the outer pair of these lines to hydrogen atoms and the inner triplet to NH_2 accounting for the small splitting (relative to the free atom value of 50.9 milliweber/m^2 for hydrogen) by the hypothesis that the dielectric constant of solid NH_3 changes the hyperfine (I·S) coupling. It is proposed that this interpretation of the spectrum is incorrect.

2. A method of heterodyne detection for EPR spectrographs is suggested which would require only one klystron instead of the two usually used. This would eliminate the AFC usually used in this type of spectrograph to maintain a constant difference in frequency between the two klystrons.

3. An experiment is proposed by which the anisotropy of β ray emission may be studied without the use of demagnetization temperatures, and employing only one counter. This experiment would make use of the Overhauser (2) effect to obtain nuclear alignment and a simultaneous pulsed nuclear resonance.

4. It is proposed that a study of the recombination of nitrogen atoms in the Broida-Pellam afterglow by means of EPR be made in order to find the relation between the recombination and the blue flashes observed on warming the afterglow.

5. Rice and Freamo (3) have found that upon condensation the products of an electric discharge through N_3H form a blue paramagnetic solid. They attribute these properties of the solid to NH radicals. It is proposed that a study of this solid be made with EPR at wavelengths of 3, 1.2, and .5 cm to check this hypothesis and determine possible zero field splitting in NH.

6. McLennan and Shrum (4) in 1924 found that solid nitrogen bombarded with cathode rays produced a green glow having an emission spectrum similar to that of the Broida-Pellam afterglow. It is proposed that McLennan's method may be easily adapted to produce free radicals for study by EPR. This method has several advantages over the X and gamma ray irradiation methods now in use.

7. It is proposed that EPR techniques may be used to study the role of free radicals in the chemistry of flames. By using low pressure one may make flame fronts of considerable thickness which may be main-

tained by a flow system inside the resonant cavity.

8. A general method for finding

$$S = \sum_{m=-I}^{I} m^n ,$$

is suggested. I is integral or half integral and n is integral.

9. Since it has been shown by Hahn (5) that the width of the echo pulse in a spin echo experiment is inversely proportional to the field gradient it is proposed that a spin echo probe would prove useful in mapping the gradient of a magnetic field directly.

10. It is proposed that rationalized M.K.S. electromagnetic units be adopted as standard in the undergraduate chemistry courses. Not only have these units been blessed with International approval but produce answers in units actually measured e.g. volts, amperes, and coulombs.

REFERENCES

1. M. S. Matheson and B. Smaller, J. Chem. Phys., 23, 521-528 (1955).
2. A. Overhauser, Phys. Rev., 92, 411- (1953).
3. F. O. Rice and M. F. Freamo, J.A.C.S., 75, 548-549 (1953).
4. J. C. McLennan and C. M. Shrum, Proc. Roy. Soc., A106, 138-149 (1924).
5. E. L. Hahn, Phys. Rev., 80, 580-594 (1950).